Published in final edited form as:

J Chromatogr B Analyt Technol Biomed Life Sci. 2015 April 15; 988: 166–174. doi:10.1016/j.jchromb.2015.02.017.

Development of a Tandem Affinity Phosphoproteomic Method with Motif Selectivity and its Application in Analysis of Signal Transduction Networks

Laura E. Herring[1], **Kyle G. Grant**[2], **Kevin Blackburn**[1], **Jason M. Haugh**[3], and **Michael B. Goshe**[1,*]

[1]Department of Molecular and Structural Biochemistry, North Carolina State University, Raleigh, North Carolina 27695-7622, United States

[2]Gene Therapy Center, University of North Carolina-Chapel Hill, Chapel Hill, North Carolina 27599-73522, United States

[3]Department of Chemical and Biomolecular Engineering, North Carolina State University, Raleigh, North Carolina 27695-7905, United States

Abstract

Phosphorylation is an important post-translational modification that is involved in regulating many signaling pathways. Of particular interest are the growth factor mediated Ras and phosphoinositide 3-kinase (PI3K) signaling pathways which, if misregulated, can contribute to the progression of cancer. Phosphoproteomic methods have been developed to study regulation of signaling pathways; however, due to the low stoichiometry of phosphorylation, understanding these pathways is still a challenge. In this study, we have developed a multi-dimensional method incorporating electrostatic repulsion-hydrophilic interaction chromatography (ERLIC) with tandem IMAC-TiO_2 enrichment for subsequent phosphopeptide identification by LC/MS/MS. We applied this method to PDGF-stimulated NIH 3T3 cells to provide over 11,000 unique phosphopeptide identifications. Upon motif analysis, IMAC was found to enrich for basophilic kinase substrates while the subsequent TiO_2 step enriched for acidophilic kinase substrates, suggesting that both enrichment methods are necessary to capture the full complement of kinase substrates. Biological functions that were over-represented at each PDGF stimulation time point, together with the phosphorylation dynamics of several phosphopeptides containing known kinase phosphorylation sites illustrate the feasibility of this approach in quantitative phosphoproteomic studies.

Corresponding author: Dr. Michael B. Goshe, Department of Molecular and Structural Biochemistry, North Carolina State University, 128 Polk Hall, Campus Box 7622, Raleigh NC 27695-7622, phone: 919.513.7740, fax: 919.515.2047, michael_goshe@ncsu.edu.

Appendix A. Supplementary data

Supplementary data associated with this article can be found, in the online version, at:

Keywords

phosphopeptide enrichment; liquid chromatography; mass spectrometry; motif analysis; pathway analysis

1. Introduction

Protein phosphorylation is among the most widespread post-translational modification (PTM) affecting almost every cellular process, including signal transduction pathways that are involved in cell proliferation, survival and differentiation. Understanding how these signaling pathways are controlled is important since misregulation contributes to the progression of cancer [1–3]. Traditionally, the phosphorylation dynamics of proteins involved in these signal transduction pathways have been elucidated using quantitative immunoblotting and other antibody-based methods [4–9]. More recently, global phosphoproteomic studies using LC/MS/MS have been implemented to study pathway regulation [10,11] and have advantages over quantitative immunoblotting such as the ability to multiplex and independence from the use of poorly characterized antibodies or those with limited specificity. However, challenges for LC/MS/MS studies including optimization of phosphopeptide enrichment protocols still remain.

Several phosphopeptide enrichment methods have been described which first use a liquid chromatography method to fractionate peptides, such as strong cation exchange (SCX) [12,13], strong anion exchange (SAX) [14], hydrophilic interaction chromatography (HILIC) [15], basic reversed-phase [16], or electrostatic repulsion-hydrophilic interaction chromatography (ERLIC) [17]. This fractionation is then followed by a phosphopeptide enrichment step [18–22]. Even though modifications to previous methods [23,24] or antibody-based phosphopeptide enrichment methods [25,26] have been developed, immobilized metal ion affinity chromatography (IMAC) [27] or TiO_2 [28] affinity enrichment are still the most widely used in phosphoproteomic analysis. With IMAC, a positively charged metal cation, such as Fe^{3+}, Zr^{4+} or Ga^{3+}, chelated to a solid-phase support noncovalently binds to a negatively charged phosphate group at low pH. While non-specific binding is minimized by washing with a low pH solution prior to phosphopeptide elution, non-specific binding of acidic peptides hinders this enrichment process. TiO_2 is a type of metal oxide affinity chromatography that has been shown to enrich for phosphopeptides more efficiently and with better selectivity than IMAC. This is accomplished by using various organic acids, such as 2,5-dihydroxybenzoic acid (DHB) and glycolic acid, to block binding of acidic peptides, leading to an increase in phosphopeptide specificity [28]. Differences in phosphopeptide populations enriched by IMAC and TiO_2 have been observed, especially with regards to the number of phosphorylation sites per peptide. IMAC enriches for multiply phosphorylated peptides more efficiently than TiO_2, while TiO_2 enriches for a higher proportion of mono-phosphorylated peptides [29,30]. Additionally, it has been argued that using IMAC results in under-representation of basophilic kinase substrates, which could lead to biases in the data and an unbalanced portrayal of the phosphoproteome [24]. The analytical merit of implementing both of these

enrichment methods, either individually or sequentially, to increase the number and variety of identified phosphopeptides has been demonstrated [29–33].

Previously we reported a method for phosphopeptide enrichment incorporating ERLIC fractionation with IMAC [34]. Using this as a basis, we optimized a multi-dimensional method using ERLIC fractionation coupled with a tandem IMAC and TiO_2 enrichment approach in order to take advantage of characteristics of both of these phosphopeptide enrichment strategies. The method was applied to PDGF responsive NIH 3T3 cells over a 120 min time course, followed by LC/MS/MS analysis using a data-dependent CID/ETD decision tree (DT) method. We demonstrated the capability of this approach to enrich for a wide variety of phosphopeptides pertaining to both basophilic and acidophilic kinase substrate motifs when compared to other methods evaluated in this study. Furthermore, the analysis of biological functions that were over-represented at each time point, as well as the phosphorylation dynamics of several phosphopeptides illustrated the feasibility of our method for use in future quantitative studies.

2. Materials and Methods

2.1 Materials

All tissue culture reagents were purchased from Invitrogen (Life Technologies, www.lifetechnologies.com). Human recombinant PDGF-BB was purchased from Peprotech (www.peprotech.com). NIH 3T3 mouse fibroblasts were obtained from American Type Culture Collection (www.atcc.org). Acetonitrile (HPLC grade) and formic acid (ACS reagent grade) were from Sigma-Aldrich (www.sigmaaldrich.com). Acetone was purchased from Thermo Fisher Scientific (www.thermofisher.com). Ammonium bicarbonate and guanidinium chloride were from Fluka (www.sigmaaldrich.com). Water was distilled and purified using a High-Q 103S water purification system (www.high-q.com). All other reagents and chemicals were purchased from Sigma-Aldrich-Fluka unless otherwise stated.

2.2 Cell Culture and Lysis

NIH 3T3 fibroblasts were cultured at 37°C with 5% CO_2 in Dulbecco's modified Eagle's medium supplemented with 10% fetal bovine serum, 2 mM l-glutamine, and the antibiotics penicillin (100 units/ml) and streptomycin sulfate (100 μg/ml). Dishes to be processed on the same day were plated with equal numbers of cells and allowed to reach 90% confluency. Cells were serum-starved for 3 h prior to no stimulation or 300 pM PDGF stimulation for 15 or 120 min. Cells were harvested and lysed as previously described [4]. A 5-fold volume of ice-cold acetone was added to each sample, vortexed, and then incubated at −20°C overnight. After centrifugation, the supernatant was discarded and the dried protein precipitate was dissolved in 50 mM ammonium bicarbonate (pH 8.2) containing 8 M urea. The total protein concentration was determined by the BCA assay (Pierce, www.piercenet.com).

2.3 Protein Digestion

Equal amounts of protein from each sample were reduced with 5 mM DTT at 56°C for 30 min and alkylated with 15 mM iodoacetamide in the dark at room temperature for 1 h. The

samples were diluted 1:8 with 50 mM ammonium bicarbonate and digested with sequencing grade trypsin (Promega, www.promega.com) at a 1:100 trypsin:protein ratio overnight at 37°C. Peptides were desalted using a Grace Prevail C18 solid-phase extraction cartridge, and the solvent was evaporated via vacuum centrifugation. Peptides were stored at −80°C until further processing.

2.4 ERLIC Fractionation

Each ERLIC separation was performed on an Agilent 1100 series HPLC system using a 4.6 × 200 mm, 5 μm particle size, 300A pore size PolyWAX LP column (PolyLC, Inc; www.polylc.com), as we previously described [34] with slight modifications. Briefly, the mobile phase consisted of (A) 20 mM ammonium formate, pH 2.2/70% acetonitrile (ACN) and (B) 300 mM ammonium formate, pH 2.2/20% ACN. After injection, an isocratic flow of 15 min at 100% A was followed by a linear gradient from 0–50% B over 20 min and a linear gradient of 50–100% B over 5 min at a flow rate of 0.75 ml/min. Fractions were collected every minute and then combined into five total fractions based on chromatographic peak intensities measured at 280 nm using a diode array detector. Each sample was dried under vacuum centrifugation and stored at −20°C until phosphopeptide enrichment.

2.5 Phosphopeptide Enrichment

The procedure for IMAC (Fe-IMAC) was as we previously described [34], with a few modifications. Briefly, nitriloacetic acid (NTA) resin (Life Technologies, www.lifetechnologies.com/) charged with 100 mM $FeCl_3$ was packed into a gel loading pipet tip made in-house containing a frit, and the resin was washed twice with 100 μl of 2% acetic acid. ERLIC fractionated peptides were resolubilized in 2% acetic acid, loaded onto the IMAC column, and washed twice with 100 μl of 2% acetic acid. The flow through and washes were collected and dried using vacuum centrifugation. A more stringent wash was performed twice with 100 μl of 74/25/1 100 mM NaCl/ACN/acetic acid (v/v/v), followed by a 100 μl wash with only water. Retained peptides were eluted with 100 μl of 5% NH_4OH, then immediately acidified to pH 3 with formic acid. The eluted peptides were dried using vacuum centrifugation, and resuspended in 0.1% formic acid for LC/MS/MS analysis. This fraction is referred to as the “IMAC fraction”.

The IMAC flow through and washes were subjected to TiO_2 enrichment using the Protea TiO_2 SpinTips Sample Prep Kit (proteabio.com) following manufacturer’s instructions. Briefly, 4 mg of TiO_2 material was used for each sample and was washed two times with 100 μl of wash solution 1. Peptides were loaded on the TiO_2 column and washed two times with 100 μl of wash solution 1, followed by two more washes with 100 μl of wash solution 2. Retained peptides were eluted with the elution solution. The eluted peptides from TiO_2 were acidified to pH 3 with formic acid, dried using vacuum centrifugation, and resuspended in 0.1% formic acid for LC/MS/MS analysis. This fraction is referred to as the “IMAC-TiO_2 fraction”. The entire sample preparation workflow is illustrated in Figure 1.

2.6 LC/MS/MS Data Acquisition

LC/MS/MS analyses were performed on an Easy nLC 1000 ultra-pressure liquid chromatograph coupled to an ETD equipped LTQ Orbitrap Elite mass spectrometer (Thermo

Scientific, www.thermoscientific.com). Samples were injected onto a PepMap C18, 5 μm, trapping column (Thermo Scientific) then separated by in-line gradient elution onto a New Objective (www.newobjective.com) Self-Pack PicoFrit column (75 μm id × 15 cm) packed in-house with 1.7 μm BEH C18 stationary phase (Waters Corporation, www.waters.com). The linear gradient for separation consisted of 5–40% mobile phase B over 60 min at a 300 nl/min flow rate, where mobile phase A was 0.1% formic acid/2% ACN in water and mobile phase B consisted of 0.1% formic acid in ACN. The Orbitrap Elite was operated in data-dependent decision tree mode [35] where the 15 most intense precursors were selected for subsequent fragmentation using optimal settings for each activation technique (illustrated in Supplementary Figure S1). Resolution for the precursor scan (*m/z* 400–2000) was set to 60,000 at *m/z* 400 with a target value of 1×10^6 ions. The MS/MS scans were acquired in the linear ion trap with a target value of 5000. The normalized collision energy was set to 35% for CID. For ETD, reaction time was set to 50 ms and supplemental activation using CID was enabled. The signal intensity threshold for triggering an MS/MS event was set to 1000. For internal mass calibration, the ion of polycyclodimethylsiloxane with *m/z* 445.120025 was used as the lock mass [36]. Monoisotopic precursor selection was enabled, and precursors with unknown charge or a charge state of 1 were excluded.

2.7 Data Analysis

Raw data files of the IMAC and IMAC-TiO_2 fractions were processed using Proteome Discoverer (PD) version 1.3 (Thermo Scientific). The non-fragment filter was used to simplify ETD spectra to remove unfragmented precursor or charge-reduced precursor peaks. Peak lists were searched against a forward and reverse *Mus musculus* UniProt database (74232 sequences) using both Mascot (Matrix Science) and Sequest (Thermo Scientific). The following parameters were used to identify tryptic peptides for protein identification: 10 ppm precursor ion mass tolerance; 0.6 Da product ion mass tolerance; up to two missed trypsin cleavage sites; carbamidomethylation of Cys was set as a fixed modification; oxidation of Met and phosphorylation of Ser, Thr, and Tyr were set as variable modifications. The percolator node was used to estimate the number of false positive identifications, and a q-value was assigned; a “high confidence” q-value of <0.01 was used to filter all results. The phosphoRS algorithm was used to measure the phosphorylation site localization probabilities [37]. Only phosphopeptides with pRS probabilities above 70% were considered for phosphorylation motif analyses, which were conducted using motif-x [38,39]. Motif-x default settings were used (with the MS/MS IPI Mouse Proteome as foreground format and as background), except the significance threshold was set to a more stringent value of 1×10^{-7} to reduce false positives. For relative quantification of specific phosphopeptides, peaks areas for each identified phosphopeptide were extracted using the peak area node in PD.

2.8 Bioinformatics Analysis

All analyses were conducted using either JMP Pro 10.0 (SAS Institute, www.sas.com) or Microsoft Excel 2010. The ClueGo plug-in [40] within Cytoscape [41] (version 3.0.2) was used to determine over-represented molecular function GO annotations and KEGG pathways. Enrichment analysis was based on two-sided minimal-likelihood test on the hypergeometric distribution. The Bonferroni step down correction was employed to adjust

p-values for statistically enriched terms (p-value of 0.1 was considered significant). Venn diagrams were generated using the Venn Diagram Plotter (PNNL, omics.pnl.gov).

3. Results and Discussion

3.1 Development of a tandem phosphopeptide enrichment strategy combining ERLIC, IMAC and TiO_2 with CID/ETD LC/MS/MS analysis

The aim of this study was to develop an optimal phosphopeptide enrichment strategy to detect phosphorylation events occurring in PDGF-stimulated fibroblasts using mass spectrometry. In order to reduce sample complexity and increase the ability to identify phosphopeptides, we coupled ERLIC with tandem IMAC/TiO_2 enrichment. ERLIC was chosen for off-line LC peptide separation since it is a combination of hydrophilic interaction and weak anion-exchange that favors retention and separation of relatively hydrophilic, negatively charged analytes such as phosphopeptides [17]. Previous studies using only ERLIC have demonstrated an enrichment of phosphopeptides [42,43]. To test this with our system, we analyzed several ERLIC fractions by LC/MS/MS and detected very few phosphopeptides (data not shown), which has also been reported in the literature [34,44]; therefore, an enrichment step after ERLIC fractionation was required.

Frequently after any type of off-line LC separation of peptides, the phosphopeptides are enriched using IMAC or TiO_2. The capacity of the IMAC or TiO_2 material can be estimated, but regardless of this, some phosphopeptides will have limited binding due to the low phosphorylation stoichiometry, as well as competition with other phosphopeptides and acidic peptides, thus precluding their identification. In order to enrich for phosphopeptides that may have not been captured when only implementing a single enrichment strategy and eventually end up in the flow-through/wash portion of the sample, a tandem phosphopeptide enrichment approach was developed. By retaining the flow-through/wash generated by one phosphopeptide enrichment method and subjecting it to a different enrichment method, it is possible to maximize the number of unique phosphopeptides identified [30].

In this study, a combination of IMAC (Fe-IMAC) and TiO_2 was chosen in order to take advantage of both phosphopeptide enrichment methods. Our order of phosphopeptide enrichment by IMAC and TiO_2 was experimentally determined by comparing the enrichment of unstimulated NIH 3T3 cell lysate digest (200 μg) using IMAC first, followed by TiO_2 enrichment of the IMAC flow-through/wash (the IMAC-TiO_2 sample) versus enriching the same amount of NIH 3T3 cell lysate digest with TiO_2 first, then using IMAC on the TiO_2 flow-through/wash (the TiO_2-IMAC sample). As shown in Supplementary Figure S2, using IMAC or TiO_2 first enriched for about the same number of phosphopeptides, but the enrichment percentage was lower for IMAC (45%) when compared to TiO_2 (80%), thus indicating that a higher level of non-specific binding was occurring with IMAC. For the second enrichment step, the IMAC-TiO_2 fraction produced more identified unique phosphopeptides than the TiO_2-IMAC fraction; therefore, the tandem enrichment order of IMAC followed by TiO_2 was used for our study. It should be noted that the IMAC-TiO_2 flow-through/wash was also analyzed, but only 44 phosphopeptides out of 4059 total peptides (1% enrichment) were identified, and thus it was excluded from subsequent analyses.

For our study, NIH 3T3 cells were stimulated with PDGF for 0, 15 and 120 min then lysed and digested with trypsin. Each lysate digest (3 mg for each time point) was separated using ERLIC to produce a total of five fractions, which were subsequently enriched for phosphopeptides with our optimized tandem IMAC/TiO_2 method (Figure 1). Although the number of ERLIC fractions was less than the typical 10 to 25 fractions generated by ERLIC or SCX for off-line peptide separations [19,22,42], the number of fractions doubles to 10 per stimulation time point (30 samples total) since each ERLIC fraction was subjected to tandem IMAC/TiO_2 enrichment. Therefore, minimizing the number of ERLIC fractions helped to reduce sample preparation and LC/MS/MS acquisition time. The list of unique phosphopeptides for all ERLIC fractions and subsequent affinity enrichment steps is presented in Supplementary Table S1.

To better identify phosphopeptides during LC/MS/MS, a data dependent DT acquisition method utilizing CID and ETD was evaluated (Supplementary Figure S3A) and implemented. After data processing, 11,310 unique phosphopeptides were identified across all 30 samples. The phosphopeptides targeted for ETD fragmentation resulted in slightly higher phosphorylation site localization probabilities (pRS probabilities) compared to phosphopeptides targeted for CID fragmentation (Supplementary Figure S3B) and about 9% of phosphorylated peptides were uniquely identified using ETD (Supplementary Figure S3C).

3.2 Enhanced phosphopeptide detection in NIH 3T3 cells using a tandem IMAC/TiO_2 enrichment approach

To evaluate the phosphopeptide enrichment strategies, all five ERLIC fractions corresponding to IMAC and IMAC-TiO_2 enrichment at each time point of PDGF stimulation were examined. A similar phosphopeptide distribution in ERLIC fractions among each corresponding IMAC and IMAC-TiO_2 sample was observed across the time course (Figure 2A). For ERLIC Fractions 1–4, a disproportionate number of phosphopeptides were enriched by IMAC compared to IMAC-TiO_2 with an exception occurring at ERLIC Fraction 2 at 15 min. However, for ERLIC Fraction 5 across all time points, the number of phosphopeptides enriched by IMAC-TiO_2 was dramatically higher than IMAC enrichment and is in stark contrast to the other four ERLIC fractions. The consistency in the level of phosphopeptide enrichment between IMAC and IMAC-TiO_2 across all time points indicates that this method is robust among ERLIC fractionated unstimulated and stimulated samples.

These observations can be explained when considering the nature of the ERLIC separation. During ERLIC, the gradient linearly increases from 20 to 300 mM ammonium formate, thus the highly acidic or multiply phosphorylated peptides elute later in the gradient and is best represented by ERLIC Fraction 5. The population of phosphopeptides detected in this fraction suggests that IMAC is less effective at enriching for acidic and/or multiply phosphorylated peptides than the subsequent TiO_2 step. To determine if non-specific binding of acidic peptides was the cause of this decrease in IMAC-enriched phosphopeptides, the non-phosphorylated peptides were examined. In ERLIC fraction 5, the number of non-phosphorylated peptides was low for both IMAC and IMAC-TiO_2 samples,

suggesting that IMAC was not enriching for highly acidic non-phosphorylated peptides at the expense of phosphopeptides. This decrease in IMAC-enriched phosphopeptides in later ERLIC fractions has been observed previously [34].

When considering all unique 11,310 phosphopeptides identified, only 23% were identified in both the IMAC and IMAC-TiO_2 fractions with more unique phosphopeptides identified in the IMAC fractions (46%) compared to the IMAC-TiO_2 fractions (31%) (Figure 2B). This relatively low overlap suggests that using a tandem IMAC/TiO_2 enrichment strategy yields more unique phosphopeptide identifications as opposed to using only IMAC or TiO_2 after the ERLIC separation. It is interesting to note that the general characteristics of the phosphopeptide populations enriched by either IMAC or IMAC-TiO_2 are different: (1) longer phosphopeptides were enriched in the IMAC-TiO_2 fractions compared to IMAC fractions and (2) the overall pI of the phosphopeptide population in the IMAC-TiO_2 fractions was lower (average pI of 4.6) than the IMAC fractions (average pI of 6).

When considering the subgroup of multiply phosphorylated peptides (Figure 3A), IMAC-TiO_2 enriched for multiply phosphorylated peptides slightly more efficiently than IMAC on the basis of enrichment percentage (17% compared to 13%), but both enrichments produced nearly the same number of unique multiply phosphorylated peptides. A closer examination of individual ERLIC fractions reveals that for ERLIC Fractions 1–4, IMAC enriched for a greater number and higher percentage of multiply phosphorylated peptides (Figure 3B) compared to IMAC-TiO_2 (Figure 3C); however, for ERLIC Fraction 5, IMAC-TiO_2 is vastly superior to IMAC. Considering that 74% of all multiply phosphorylated peptides identified by IMAC-TiO_2 were in ERLIC Fraction 5, it can be concluded that IMAC-TiO_2 is able to enrich for larger, highly acidic multiply phosphorylated peptides better than IMAC. Overall, these data suggest that there is complementarity between the IMAC and IMAC-TiO_2 phosphopeptide enrichment methods as applied to ERLIC separated peptide fractions.

3.3 IMAC and IMAC-TiO2 enrich for different phosphorylation motifs

Although the tandem affinity enrichment of IMAC and IMAC-TiO_2 of ERLIC fractionated peptides appear to favor basic and acidic phosphopeptides, respectively, the overall ratio of pS:pT:pY between these two enriched fractions was very similar: 84:14:2 and 87:12:1, respectively. In order to provide a more definitive comparison to assess the basic and acidic phosphopeptide preferences between the two enrichment methods, phosphorylation motif analysis was conducted using motif-x [38,39].

As shown in Figure 4A, IMAC and IMAC-TiO_2 enrich for noticeably different pS motifs. The top pS motifs for the IMAC fractions were those with an overall neutral or positive charge, while the top motifs for the IMAC-TiO_2 fractions were those with an overall negative charge. These results clearly indicate that the enrichment of ERLIC fractionated peptides: IMAC-TiO_2 is better at enriching for acidic phosphopeptides than IMAC. For pT motifs (Figure 4B), IMAC and IMAC-TiO_2 were able to enrich for very similar proline-directed kinase motifs. Motif-x analysis was also conducted for pY motifs, but the low number of phosphopeptides (~100) used in the search precluded the identification of any motifs. To better understand these findings, the biological significance of the identified kinase motifs was examined.

Many of the kinase motifs enriched by our ERLIC-based tandem IMAC/TiO_2 affinity approach have been biologically well-characterized. The RRxpS motif is found in basophilic substrates that are phosphorylated by Arg-directed or AGC-family kinases, such as PKA, PKG, PKC, RSK and Akt, which all play important roles in signal transduction [45]. The (pS/T)PxK/R motifs are found in MAPK/CDK substrates, which are involved in cell proliferation and cell cycle control [46]. Some substrates for Akt, which plays a role in mediating critical cellular responses, are known to contain the RxRxxpS/T motif [47]. The pS motifs such as pS(D/E)xE and pSxDxExE, are found in acidophilic substrates phosphorylated by CK2. CK2 is a highly conserved, ubiquitous, and constitutively active Ser/Thr protein kinase with hundreds of targets that are involved in a variety of cellular processes such as cell cycle progression, apoptosis, transcription, inflammation, and DNA damage response [46,48]. It is widely known that the majority of peptides are phosphorylated by proline-directed kinases [38,49], thus are probably highly abundant relative to some other motifs. Two of these ubiquitous motifs (RxxpSP and pSPxK) were found in both IMAC and IMAC-TiO_2 samples suggesting that the amount of IMAC resin used may not provide the necessary binding capacity to enrich for all phosphopeptides containing these motifs, and thus those not completely retained are further captured by subsequent TiO_2 affinity.

A previous study also found that TiO_2 has a tendency to isolate acidic phosphopeptides when compared to IMAC without any prior fractionation step [29] while another study found no bias in phosphopeptides enriched from complex peptide mixtures by IMAC and TiO_2 [50]. To determine if the motif selectivity we observed was a result of ERLIC fractionation, motif-x analysis was conducted for LC/MS/MS identified peptides enriched from an unstimulated NIH 3T3 cell lysate using only IMAC or TiO_2 enrichment. An almost identical mixture of both acidophilic and basophilic kinase substrate motifs were identified between the IMAC and TiO_2 samples (Supplementary Figure S4), indicating that not as many unique motifs were identified if only IMAC or TiO_2 enrichment were performed without prior ERLIC fractionation. Interestingly, if an additional enrichment step using either TiO_2 on the IMAC flow-through/wash or IMAC on the TiO_2 flow-through/wash was performed, enrichment of only motifs associated with basophilic kinase substrates was observed These data indicate that a significant enrichment of motifs associated with acidophilic kinase substrates occurs only if ERLIC fractionation is used prior to IMAC/TiO_2 tandem enrichment. In comparison to a previous study [42], ERLIC alone produced better coverage of acidophilic kinase substrates compared to SCX/IMAC, but SCX/IMAC produced better coverage of basophilic kinase substrates, which is consistent with the chemical basis of the separation prior to IMAC. Overall, these findings suggest that our method of combining ERLIC with IMAC/TiO_2 tandem affinity increases the phosphopeptide enrichment efficiency of both acidophilic and basophilic kinase substrates.

3.4 Biological Effects upon PDGF Stimulation Time Course

To obtain a better understanding of the signaling pathways modulated by PDGF stimulation, the Cytoscape plugin, ClueGO, was used to determine the over-represented KEGG pathways within the total phosphoproteomic dataset (Figure 5). The pathways of interest, which include the well-characterized MAPK, Ras, and the PI3K-Akt pathways, were significantly

represented in the dataset. Intriguingly, the mTOR pathway, which is known to be involved in crosstalk with the PI3K-Akt and Ras pathways [51–53], was the most over-represented pathway in the dataset. Other interesting over-represented pathways include the cell cycle, focal adhesion signaling, and the p53 pathway. Several of the detected phosphorylation sites within proteins involved in these pathways are of unknown function (e.g., Ser198 on Rin1) or are completely novel sites (e.g., Ser1000 on Abl2), suggesting the possibility of novel regulatory features within the PDGF signaling network.

In terms of overall phosphorylation identification (Supplementary Figure S5), the overlap of phosphopeptides in all three sample sets (0, 15 and 120 min) was 21% whereas the phosphoprotein overlap was 45%, indicating that numerous phosphorylation events are occurring upon PDGF stimulation. The over-represented molecular function GO terms for each PDGF stimulation time point are shown in Supplementary Figure S6. It is evident that some functions are more prevalent during specific PDGF stimulation time points. For example, kinase activity and histone binding were over-represented at 15 min whereas cytoskeletal binding and phosphatase activity were over-represented at 120 min. Very few phosphoregulated functions were over-represented at 0 min, consistent with quiescent cell state.

To explore the data further, the phosphorylation dynamics of specific phosphopeptides corresponding to proteins in the Ras and PI3K signaling pathways were calculated (Supplementary Figure S7) and compared to previously published results. The ERK2 phosphorylation sites pT183 and pY185 and the MEK1/2 phosphorylation site pS222 both displayed transient phosphorylation kinetics which are consistent with previously published immunoblot data [5,6]. Raf-1, which is phosphorylated by ERK1/2 at several residues including the identified pS642 site [54], clearly demonstrated a sustained increase in activation over time. A similar trend was previously observed in immunoblot analysis of other Raf-1 sites phosphorylated by ERK1/2 [6]. These results suggest that the multidimensional phosphopeptide enrichment method presented here could be a viable approach for future quantitative studies.

4. Conclusions

In this study, a phosphopeptide enrichment strategy that combines ERLIC and tandem IMAC-TiO_2 enrichment was developed and applied to PDGF-stimulated NIH 3T3 cells. We determined that phosphopeptide enrichment using IMAC followed by TiO_2 enrichment was the optimal order of enrichment. When applied to ERLIC fractions, the level of phosphopeptide enrichment was consistent between IMAC and IMAC-TiO_2 across all time points suggesting that this method is reliable even for comparisons among unstimulated and stimulated samples. Furthermore, the enrichment strategy yielded a wide variety of phosphorylation motifs suggesting that IMAC-TiO_2 tandem affinity is needed to obtain the full complement of kinase substrates. It should be noted that the number of phosphopeptides identified could vary greatly depending upon the specific IMAC (e.g., implementing metal ions other than Fe^{3+}) and TiO_2 materials and protocols used, tissue or cell type, and other sample preparation variables required for a particular study. However, the motif selectivity displayed should still be observed for other systems using our ERLIC/IMAC/TiO_2 approach.

Based on GO annotation, specific molecular functions were over-represented at each time point, indicating that PDGF stimulation induces phosphorylation changes in a variety of proteins, not just those in the Ras and PI3K pathways. The phosphorylation changes for a few well-characterized proteins were calculated, suggesting that quantitative data can be obtained using our current approach. Given the importance of protein phosphorylation in cell regulation, the ERLIC and tandem IMAC-TiO_2 phosphopeptide enrichment approach presented here should be useful for future quantitative studies to further improve our understanding of signal transduction networks.

Supplementary Material

Refer to Web version on PubMed Central for supplementary material.

Acknowledgements

This work was supported by NIH grant R01GM088987 and NSF grant DBI-1126244.

References

1. Manning G, Plowman GD, Hunter T, Sudarsanam S. Trends Biochem. Sci. 2002; 27:514–520. [PubMed: 12368087]
2. Dhillon AS, Hagan S, Rath O, Kolch W. Oncogene. 2007; 26:3279–3290. [PubMed: 17496922]
3. Lemmon MA, Schlessinger J. Cell. 2010; 141:1117–1134. [PubMed: 20602996]
4. Park CS, Schneider IC, Haugh JM. J. Biol. Chem. 2003; 278:37064–37072. [PubMed: 12871957]
5. Wang C-C, Cirit M, Haugh JM. Mol. Syst. Biol. 2009; 5:246–257. [PubMed: 19225459]
6. Cirit M, Wang C-C, Haugh JM. J. Biol. Chem. 2010; 285:36736–36744. [PubMed: 20847054]
7. Cirit M, Haugh JM. Biochem. J. 2012; 441:77–85. [PubMed: 21943356]
8. Birtwistle MR, Hatakeyama M, Yumoto N, Ogunnaike BA, Hoek JB, Kholodenko BN. Mol. Syst. Biol. 2007; 3:144–160. [PubMed: 18004277]
9. Chen WW, Schoeberl B, Jasper PJ, Niepel M, Nielsen UB, Lauffenburger DA, Sorger PK. Mol. Syst. Biol. 2009; 5:239–258. [PubMed: 19156131]
10. Olsen JV, Blagoev B, Gnad F, Macek B, Kumar C, Mortensen P, Mann M. Cell. 2006; 127:635–648. [PubMed: 17081983]
11. Brill LM, Xiong W, Lee K-B, Ficarro SB, Crain A, Xu Y, Terskikh A, Snyder EY, Ding S. Cell Stem Cell. 2009; 5:204–213. [PubMed: 19664994]
12. Peng J, Elias JE, Thoreen CC, Licklider LJ, Gygi SP. J. Proteome Res. 2003; 2:43–50. [PubMed: 12643542]
13. Beausoleil SA, Jedrychowski M, Schwartz D, Elias JE, Villén J, Li J, Cohn MA, Cantley LC, Gygi SP. Proc. Natl. Acad. Sci. 2004; 101:12130–12135. [PubMed: 15302935]
14. Han G, Ye M, Zhou H, Jiang X, Feng S, Jiang X, Tian R, Wan D, Zou H, Gu J. Proteomics. 2008; 8:1346–1361. [PubMed: 18318008]
15. McNulty DE, Annan RS. Mol. Cell. Proteomics. 2008; 7:971–980. [PubMed: 18212344]
16. Mertins P, Qiao JW, Patel J, Udeshi ND, Clauser KR, Mani DR, Burgess MW, Gillette MA, Jaffe JD, Carr SA. Nat. Methods. 2013; 10:634–637. [PubMed: 23749302]
17. Alpert AJ. Anal. Chem. 2008; 80:62–76. [PubMed: 18027909]
18. Hoffert JD, Knepper MA. Anal. Biochem. 2008; 375:1–10. [PubMed: 18078798]
19. Villén J, Gygi SP. Nat. Protoc. 2008; 3:1630–1638. [PubMed: 18833199]
20. Macek B, Mann M, Olsen JV. Annu. Rev. Pharmacol. Toxicol. 2009; 49:199–221. [PubMed: 18834307]

21. Grimsrud PA, Swaney DL, Wenger CD, Beauchene NA, Coon JJ. ACS Chem. Biol. 2010; 5:105–119. [PubMed: 20047291]
22. Zarei M, Sprenger A, Metzger F, Gretzmeier C, Dengjel J. J. Proteome Res. 2011; 10:3474–3483. [PubMed: 21682340]
23. Iliuk AB, Martin Va, Alicie BM, Geahlen RL, Tao WA. Mol. Cell. Proteomics. 2010; 9:2162–2172. [PubMed: 20562096]
24. Zhou H, Low TY, Hennrich ML, van der Toorn H, Schwend T, Zou H, Mohammed S, Heck AJR. Mol. Cell. Proteomics. 2011; 10:M110.006452.
25. Rush J, Moritz A, Lee KA, Guo A, Goss VL, Spek EJ, Zhang H, Zha X-M, Polakiewicz RD, Comb MJ. Nat. Biotechnol. 2005; 23:94–101. [PubMed: 15592455]
26. Graves LM, Duncan JS, Whittle MC, Johnson GL. Biochem. J. 2013; 450:1–8. [PubMed: 23343193]
27. Ficarro SB, McCleland ML, Stukenberg PT, Burke DJ, Ross MM, Shabanowitz J, Hunt DF, White FM. Nat. Biotechnol. 2002; 20:301–305. [PubMed: 11875433]
28. Larsen MR, Thingholm TE, Jensen ON, Roepstorff P, Jørgensen TJD. Mol. Cell. Proteomics. 2005; 4:873–886. [PubMed: 15858219]
29. Bodenmiller B, Mueller LN, Mueller M, Domon B, Aebersold R. Nat. Methods. 2007; 4:231–237. [PubMed: 17293869]
30. Thingholm TE, Jensen ON, Robinson PJ, Larsen MR. Mol. Cell. Proteomics. 2008; 7:661–671. [PubMed: 18039691]
31. Yue X-S, Hummon AB. J. Proteome Res. 2013; 12:4176–4186. [PubMed: 23927012]
32. Zhang X, Ye J, Jensen ON, Roepstorff P. Mol. Cell. Proteomics. 2007; 6:2032–2042. [PubMed: 17675664]
33. Engholm-Keller K, Birck P, Størling J, Pociot F, Mandrup-Poulsen T, Larsen MR. J. Proteomics. 2012; 75:5749–5761. [PubMed: 22906719]
34. Chien K, Liu H, Goshe MB. J. Proteome Res. 2011; 10:4041–4053. [PubMed: 21736374]
35. Swaney DL, Mcalister GC, Coon JJ. Nat. Methods. 2008; 5:959–964. [PubMed: 18931669]
36. Olsen JV, de Godoy LMF, Li G, Macek B, Mortensen P, Pesch R, Makarov A, Lange O, Horning S, Mann M. Mol. Cell. Proteomics. 2005; 4:2010–2021. [PubMed: 16249172]
37. Taus T, Köcher T, Pichler P, Paschke C, Schmidt A, Henrich C, Mechtler K. J. Proteome Res. 2011; 10:5354–5362. [PubMed: 22073976]
38. Schwartz D, Gygi SP. Nat. Biotechnol. 2005; 23:1391–1398. [PubMed: 16273072]
39. Chou MF, Schwartz D. Biological Sequence Motif Discovery Using Motif-X. 2011
40. Bindea G, Mlecnik B, Hackl H, Charoentong P, Tosolini M, Kirilovsky A, Fridman W-H, Pagès F, Trajanoski Z, Galon J. Bioinformatics. 2009; 25:1091–1093. [PubMed: 19237447]
41. Shannon P, Markiel A, Ozier O, Baliga NS, Wang JT, Ramage D, Amin N, Schwikowski B, Ideker T. Genome Res. 2003; 13:2498–2504. [PubMed: 14597658]
42. Gan CS, Guo T, Zhang H, Lim SK, Sze SK. J. Proteome Res. 2008; 7:4869–4877. [PubMed: 18828627]
43. Zhang H, Guo T, Li X, Datta A, Park JE, Yang J, Lim SK, Tam JP, Sze SK. Mol. Cell. Proteomics. 2010; 9:635–647. [PubMed: 20047950]
44. Hao P, Guo T, Li X, Adav SS, Yang J, Wei M, Sze SK. J. Proteome Res. 2010; 9:3520–3526. [PubMed: 20450224]
45. Pearce LR, Komander D, Alessi DR. Nat. Rev. Mol. Cell Biol. 2010; 11:9–22. [PubMed: 20027184]
46. Alexander J, Lim D, Joughin Ba, Hegemann B, Hutchins JRa, Ehrenberger T, Ivins F, Sessa F, Hudecz O, Nigg Ea, Fry AM, Musacchio A, Stukenberg PT, Mechtler K, Peters J-M, Smerdon SJ, Yaffe MB. Sci. Signal. 2011; 4:ra42. [PubMed: 21712545]
47. Manning BD, Cantley LC. Cell. 2007; 129:1261–1274. [PubMed: 17604717]
48. Meggio F, Pinna La. FASEB J. 2007; 17:349–368. [PubMed: 12631575]
49. Cesaro, L.; Salvi, M. Protein Kinase CK2. Pinna, LA., editor. John Wiley & Sons; 2013. p. 117-129.

50. Kettenbach AN, Wang T, Faherty BK, Madden DR, Knapp S, Bailey-Kellogg C, Gerber Sa, et al. Chem. Biol. 2012; 19:608–618. [PubMed: 22633412]
51. Dunlop EA, Tee AR. Cell. Signal. 2009; 21:827–835. [PubMed: 19166929]
52. Laplante M, Sabatini DM. J. Cell Sci. 2009; 122:3589–3594. [PubMed: 19812304]
53. Zoncu R, Efeyan A, Sabatini DM. Nat. Rev. Mol. Cell Biol. 2011; 12:21–35. [PubMed: 21157483]
54. Dougherty MK, Müller J, Ritt DA, Zhou M, Zhou XZ, Copeland TD, Conrads TP, Veenstra TD, Lu KP, Morrison DK. Mol. Cell. 2005; 17:215–224. [PubMed: 15664191]

Highlights

- Developed a novel ERLIC-IMAC-TiO_2 phosphoproteomic enrichment approach.
- Applied to PDGF-responsive cells, yielding 11,000+ phosphopeptide identifications.
- Identified several enrichment method-specific phosphorylation motifs.
- Many biological pathways including MAPK and mTOR were over-represented in the data.

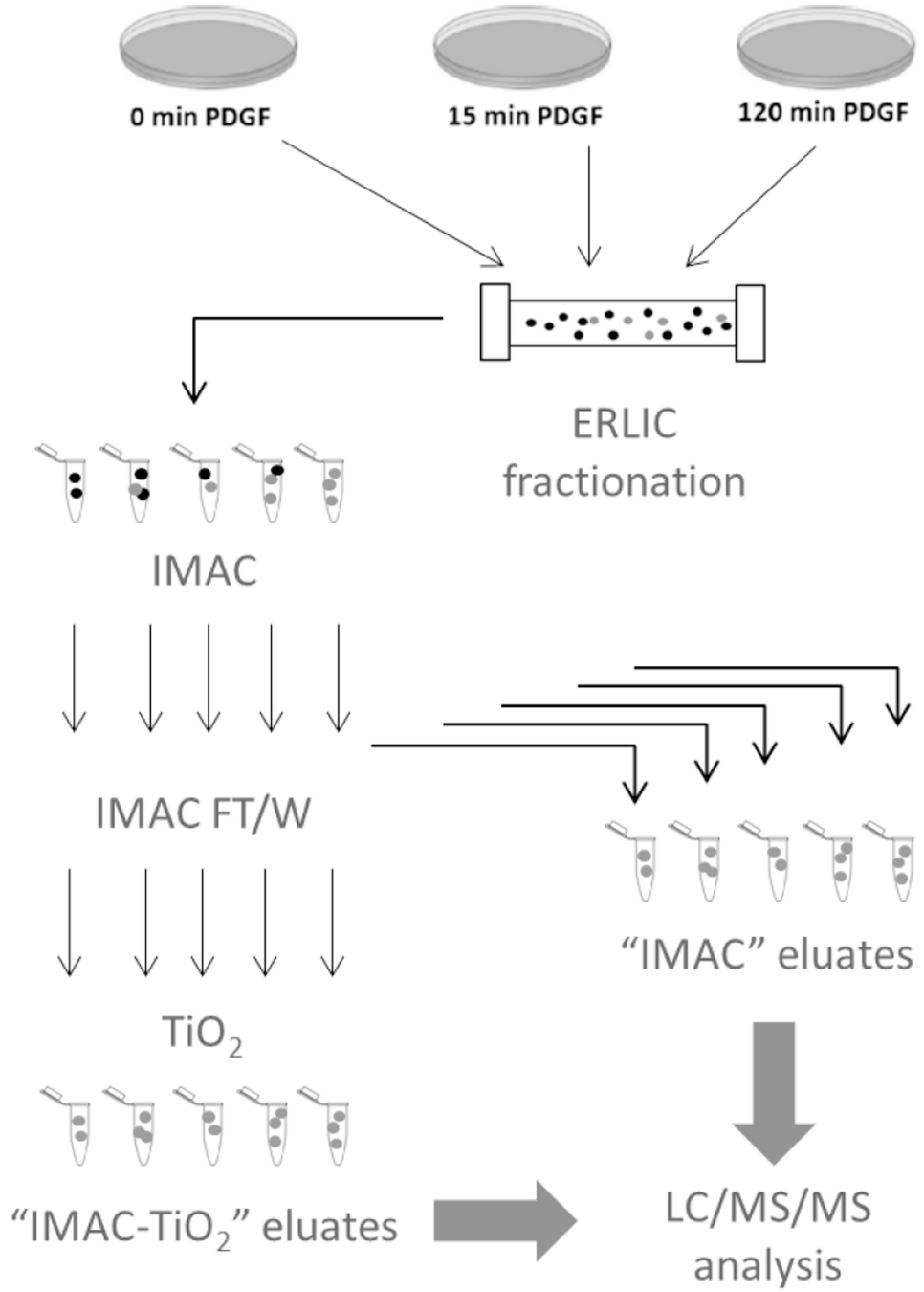

Figure 1.

Experimental workflow. NIH 3T3 cells were stimulated with 300 pM PDGF for 0, 15, and 120 min, then harvested. Each lysate (3 mg) was denatured, reduced, alkylated, digested with trypsin, then fractionated using ERLIC. Selected ERLIC fractions were pooled to generate five fractions per stimulation time point, and each ERLIC fraction was subsequently enriched for phosphopeptides using IMAC. The IMAC eluate for each fraction per time point was set aside, while the IMAC flow-through/wash (FT/W) was subjected to further phosphopeptide enrichment using TiO_2. LC/MS/MS analysis of the IMAC eluate

(referred to as the IMAC fraction) and the TiO_2 eluate from the IMAC FT/W (referred to as the IMAC-TiO_2 fraction) was performed using an Orbitrap Elite system implementing CID/ETD decision tree (DT) acquisition analysis.

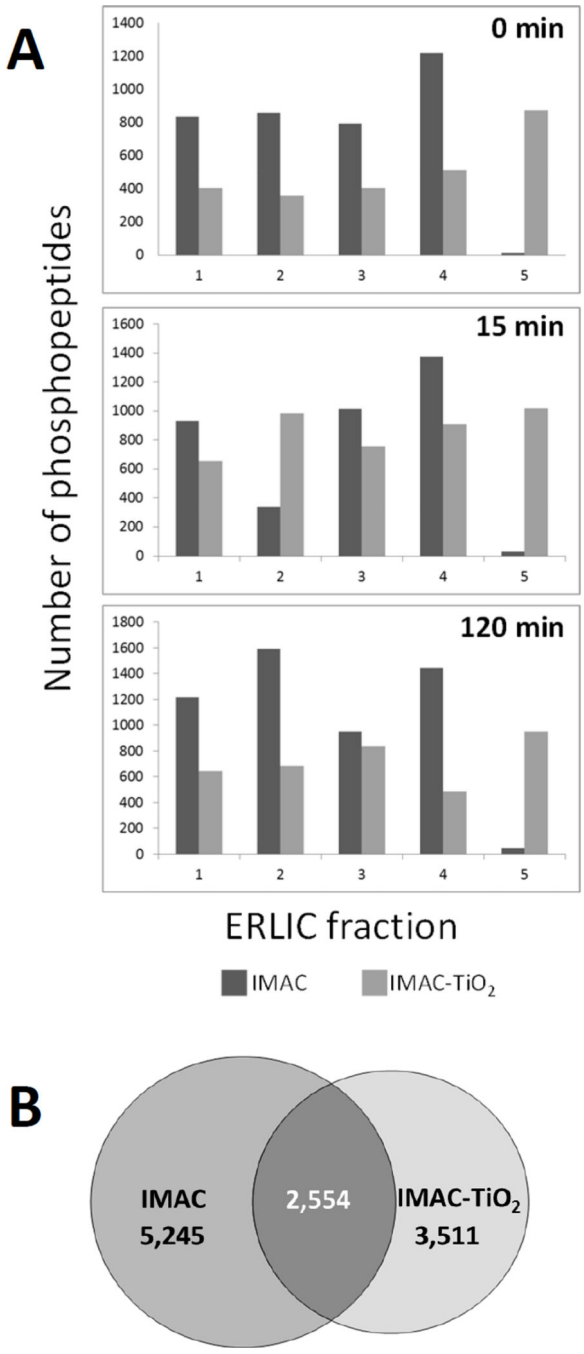

Figure 2.

Distribution of phosphopeptides detected in the IMAC and IMAC-TiO_2 samples for PDGF-stimulated NIH 3T3 cells. (A) Number of phosphopeptides identified in each IMAC and IMAC-TiO_2 sample for each stimulation time point and ERLIC fraction. (B) A Venn diagram of unique phosphopeptides identified in the IMAC and IMAC-TiO_2 samples. "IMAC" samples were generated by enriching each of the five ERLIC fractions using IMAC, and "IMAC-TiO_2" samples were generated by enriching each IMAC flow-through/wash using TiO_2.

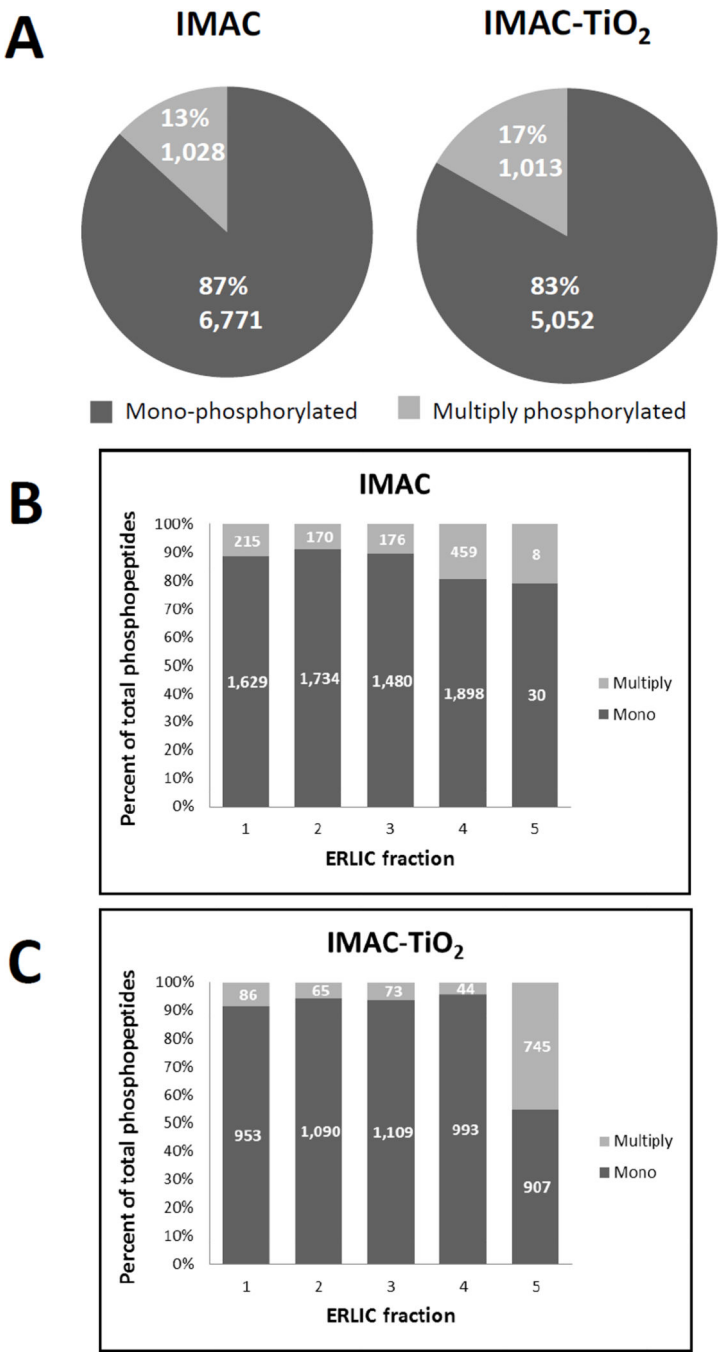

Figure 3.

Assessment of multiply-phosphorylated peptides. (A) Pie charts illustrating the number and percentage of monophosphorylated and multiply phosphorylated peptides identified in the IMAC and IMAC-TiO_2 samples. The distribution of the percentage and number of mono- and multiply-phosphorylated peptides identified in each individual ERLIC fraction across all time points for the (B) IMAC and (C) IMAC-TiO_2 fractions. "IMAC" samples were generated by enriching each of the five ERLIC fractions using IMAC, and "IMAC-TiO_2" samples were generated by enriching each IMAC flow-through/wash using TiO_2.

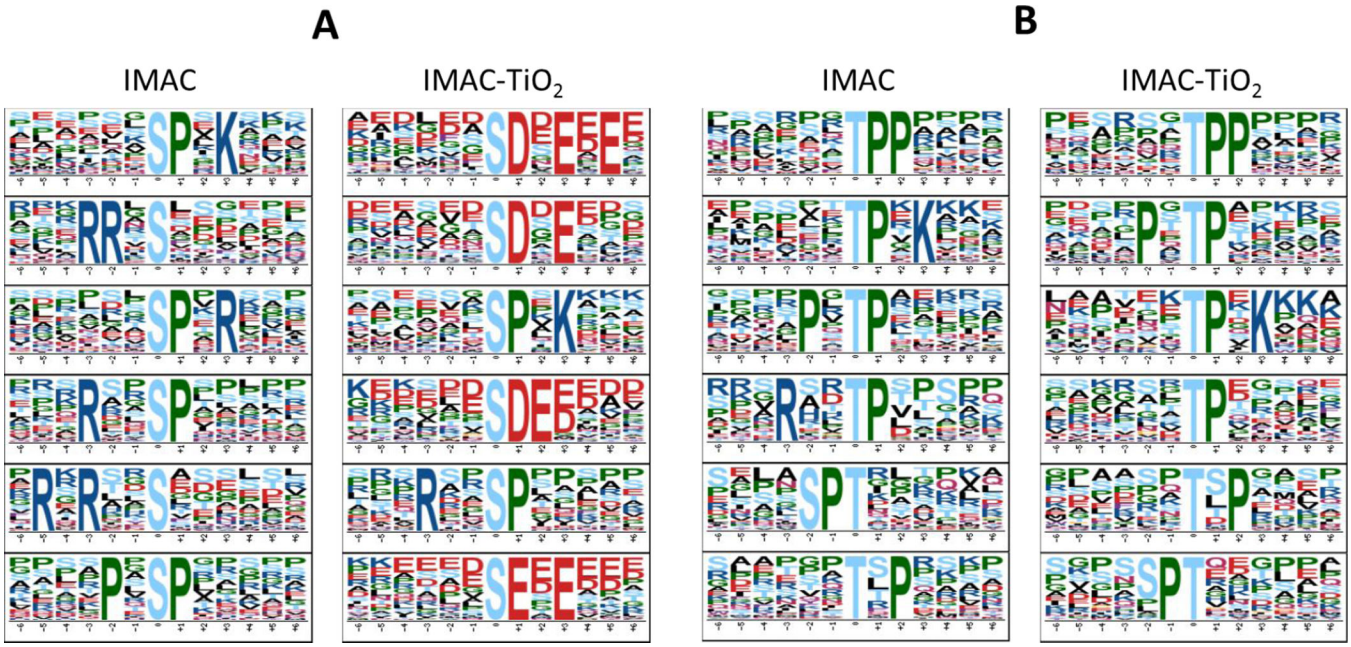

Figure 4.

Phosphorylation motif analyses of phosphopeptides identified in PDGF-stimulated NIH 3T3 cells across all time points using motif-x. Phosphopeptides with at least a 70% site localization confidence score (pRS of 0.7) were used for motif-x analysis. Of the 11,310 unique phosphopeptides identified in all fractions and time points, 7,145 have a pRS probability ≥ 0.7. The top six phosphorylation motifs generated for (A) phosphoserine (pS) and (B) phosphothreonine (pT) in the IMAC and IMAC-TiO_2 fractions are presented (top to bottom) according to motif score and fold increase. “IMAC” samples were generated by enriching each of the five ERLIC fractions using IMAC, and “IMAC-TiO_2” samples were generated by enriching each IMAC flow-through/wash using TiO_2.

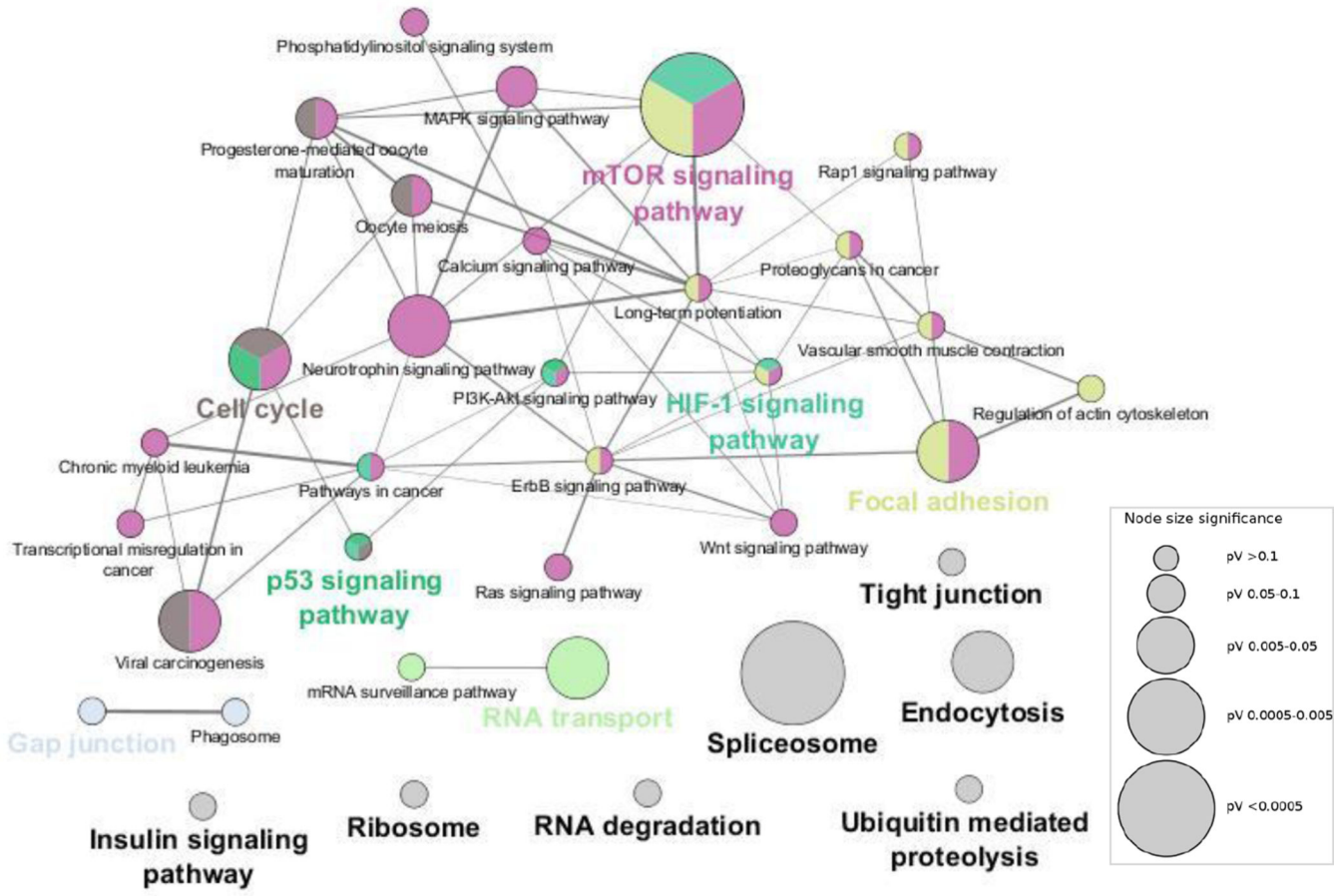

Figure 5.

KEGG pathway analysis of all identified phosphoproteins. The ClueGO plugin within Cytoscape was used to determine which KEGG pathways were over-represented in the total dataset. The size of the nodes reflects the statistical significance of the terms. The kappa score indicates the relationship between terms according to their overlapping genes and was set to the default of 0.4. The most representative term (based on the highest percentage of identified proteins per term) in a group is used as the group name. Only protein groups considered relevant are shown.